

Updated estimates of abundance for humpback whale breeding stock C3 off Madagascar, 2000-2006.

SALVATORE CERCHIO^{1,2,3}, PETE ERSTS^{1,4}, CRISTINA POMILLA^{1,2,3}, JACQUELINE LOO^{1,7}, YVETTE RAZAFINDRAKOTO^{1,5}, MATT LESLIE^{1,2}, NORBERT ANDRIANRIVELO^{1,5}, GIANNA MINDON^{6,7}, JENNIFER DUSHANE^{1,8}, ANITA MURRAY^{1,8}, TIM COLLINS^{1,6} AND HOWARD ROSENBAUM^{1,2}

¹ *Wildlife Conservation Society, Ocean Giants Program, 2300 Southern Blvd., Bronx, NY 10350-1088, USA.*

² *American Museum of Natural History, Sackler Institute for Comparative Genomics, 68th Street and Central Park West, New York, NY 10023, USA.*

³ *New York University, Department of Biology, 1008 Silver Center, 100 Washington Square East, New York, NY 10003-5577, USA.*

⁴ *American Museum of Natural History, Center for Biodiversity and Conservation, 68th Street and Central Park West, New York, NY 10023, USA.*

⁵ *Wildlife Conservation Society, Madagascar Country Program, B.P. 7400, Antananarivo, Madagascar.*

⁶ *Environment Society of Oman P.O. Box. 3844, P.C. 112, Ruwi Sultanate of Oman*

⁷ *University of Malaysia Sarawak, Piasau 60, Miri 87008, Sarawak*

⁸ *Columbia University, Department of Conservation Biology, New York, NY, USA.*

ABSTRACT

We report estimations of abundance for C3, Madagascar, using identification photographs of tail flukes and multi-locus microsatellite genotypes collected in Antongil Bay from 2000-2006. Recaptures were generally sparse, and capture probability low. A series of different models were used to estimate abundance including closed and open population models. Closed models included: Chapman's modified Petersen applied to consecutive pairs of years; close models formulated in Program MARK to relax various assumptions on probability of capture; and closed models in MARK that allow for mis-identification to account for genotyping error in genotypic data. As an open population model we used the Pradel formulated in Program mark to estimated survival, realized growth rate and capture probability, the latter of which was used to secondarily estimate abundance. The primary concerns affecting accuracy are heterogeneity of capture probability introduced by the consistent timing of capture of individuals, the small sample size relative to population size (low probability of capture), the potential for bias due to closure violations in the closed capture models, and the fit of the data to the Pradel model. Recognizing these important caveats, we recommend the use of two models to bracket the bounds of abundance for the population. As a lower bound estimate, we recommend either the Pradel unconstrained model estimate of 4936, CV=0.44, 95% confidence interval of 2137-11692, or the genotypic data, closed model, sex-aggregated weighted average estimate of 6951, CV=0.33, 95% confidence interval of 2509-11394. As an upper bound estimate, we recommend the Pradel model, photographic data of 8169, CV=0.44, 95% confidence interval of 3476-19497

INTRODUCTION

Humpback whales (*Megaptera novaeangliae*) in the southern hemisphere are distributed in circumpolar high latitudes during the austral summer and migrate to discrete or semi-discrete low latitude breeding areas in the austral winter. Population structure and status in the breeding areas is currently the focus of ongoing research (Pomilla 2005, Pomilla et al. 2006, Rosenbaum et al. 2006) as is the relationship of specific breeding regions and feeding areas. The International Whaling Commission (IWC) currently designates seven breeding stocks (populations) labeled A through G, ranging from the western South Atlantic eastward to the eastern South Pacific. The breeding population that winters in the western Indian Ocean is considered Breeding Stock C, and is distributed primarily from the eastern coastal waters of

South Africa to Kenya, off the islands of the Mozambique Channel, and the coastal waters of Madagascar.

Best et al. (1998) proposed three potential subpopulations and migratory corridors of humpback whales in the western Indian Ocean, based upon historical whaling records, land based observations of migrations, and shipboard surveys. IWC delineation of Breeding Stock C is consequently divided into three sub-regions: C1, wintering off the east coast of South Africa to Mozambique; C2, a group that potentially migrates up the Mozambique Channel to winter grounds in the Comoros Islands; and C3, wintering in the coastal waters of Madagascar (Best et al. 1997, 1998, Rosenbaum et al. 1997). The C3 sub-region has been investigated primarily in the semi-protected waters of Antongil Bay in the northeast of Madagascar (Rosenbaum et al. 1997; Rosenbaum 2003). Here we present an analysis and assessment of population abundance for the Madagascar breeding assemblage of humpback whales using individual identification photographs and microsatellite multi-locus genotypes. We discuss potential biases affecting these estimates, particularly related to migratory behavior and timing of individual whales, as well as their geographic or population level significance.

METHODS

Data used in this study were collected on the breeding area of Antongil Bay, Madagascar (Fig. 1) during the austral winters of 2000 through 2006. Antongil Bay, in the northeastern corner of Madagascar, is a shallow, semi-protected bay that extends approximately 60km northward from the mouth of the bay and is on average approximately 30km in width. Humpback whales can be observed in Antongil generally from June to October with the highest concentrations occurring in July through early September (Rosenbaum et al. 1997). Behaviors widely accepted to indicate breeding activity are regularly observed in Antongil Bay, as are females with young calves, and thus the bay is considered a breeding area for the western Indian Ocean population (Rosenbaum et al. 1997). The degree to which the bay represents an endpoint “destination” for migratory whales with high residency, versus a “stopover” point with relatively transient residency is as yet undetermined.

Individual identification photographs and skin samples for genetic identifications used in this analysis were collected from 2000 to 2006. Effort was relatively consistent each year from July to September (Table 1) with the exception of 2002, which was an anomalously short season due to political upheaval in Madagascar. Standard procedures were used for identification photography using primarily Nikon D1 digital cameras. Photographs were collected of both sides of the dorsal fin as well as the ventral tail flukes whenever possible, however recapture analysis of only tail flukes are reported here. Skin samples were collected using biopsy dart procedure (Lambertsen 1987) or, when available, as sloughed skin, and stored in 95% EtOH until processed.

Photographic comparison procedure. Whenever possible a single photograph was chosen to represent the flukes of an individual for a single day. Photographs were first compared within each year to establish within-year sample size of individuals and within-year recaptures. Between-year comparisons were then conducted starting with the first two years and sequentially comparing each subsequent year to the reconciled catalogue of all previous years. All photographs used in the comparison were rated for quality in three separate categories: *photographic*, which included focus, exposure, contrast and pixilation of digital images; *orientation*, which included angle of the flukes in the horizontal and vertical planes, amount of the flukes above water, and obstruction by splash; and *distinctiveness*, which was an intrinsic characteristic of the fluke involving the uniqueness of the pattern and degree of scarring (although this was inevitably influenced by photographic and orientation quality). Quality was rated on a five-level scale: excellent, good, fair, poor, and not useable. Flukes were also rated on the proportion of the fluke that was showing above the water plane as whole, left fluke only, right fluke only, trailing edge or leading edge. By defined protocol the latter four categories (essentially partial flukes) could only receive a fair,

poor or not useable quality rating in orientation. Flukes of all qualities were compared and used for assessing recapture rates of individuals within season and temporal characteristics of individual captures. In mark-recapture statistical procedures for the estimation of population abundance, we used only flukes with quality of fair or better in photographic and orientation categories. Photographs of only the right or left fluke were also eliminated from the sample since they cannot be compared to each other.

Genotypic comparison procedure. The genetic capture-recapture approach is based on the resolution of unique genetic profiles to permit unambiguous identification of individuals (Palsbøll et al. 1997). Total genomic DNA was extracted from the epidermal layer of biopsies or sloughed skin, using standard Phenol/Chloroform extraction method or using DNAeasy tissue kit (Qiagen). The samples were genotyped using 10 cetacean microsatellite markers selected from literature, and sex for each sampled individual determined using sex-specific molecular marker methods (Pomilla 2005). A detailed description of molecular methodology, quality control protocols and statistical analyses of genetic variation can be found in Pomilla & Rosenbaum (2006).

The average probability of different random individuals in the population sharing the same genotype by chance (Probability of Identity, PI) was estimated to evaluate the reliability of the genetic tagging based on the number of loci used. Duplicate samples were detected from genotype identity using the Microsoft Excel add-in GENALEX package version 5.1 (Peakall and Smouse, 2001). Additionally, for all samples with matching genotypes that represented putative recaptures between years, genotype probability (GP) was generated separately for the specific genotype. The genotype probability estimates the probability of a random match to a given specific genotype in the given population. PI and GP were estimated using the Microsoft Excel add-in mentioned above.

Genotyping error was assessed by the replicate processing of 182 samples, accounting for 16.2% of the total sample (Pompanon et al, 2005). Locus-specific error rates were estimated by the proportion of single locus genotypes with at least one allelic mismatch in the replicate sample, for each locus. Genotypic error rate was estimated in two manners: the observed genotypic error rate, or proportion of multi-locus genotypes with an allelic mismatch at one or more loci; and the predicted genotypic error rate, based upon the estimated locus-specific error rates.

Abundance estimation procedures. Abundance estimates were generated using several combinations of sample years and estimation models. Both closed and open population capture-recapture models were employed. Pair-wise estimates were generated using the Chapman's modified Petersen model (Begon 1979, Hammond 1986) and each consecutive pair of sample years. The Program MARK (White & Burnham 1999) was used to generate estimates from multiple years of data applying closed capture likelihood models. Program MARK allows the construction of models that relax the assumption of equal probability of capture in several manners. For each dataset, several models were run, including the null model (M_0), variation of capture probability with sampling occasion (time, M_t), individual (heterogeneity, M_h), and time in combination with individual (M_{th}). Support for models was assessed and models ranked within MARK using information theory and comparison of correct Akaike's Information Criteria (AIC_c) values (Burnham & Anderson 2002). Models that vary probability of capture and recapture periods (behavior, M_b) were not included as these models uniformly provided nonsensical results and were a poor fit to the data. MARK models heterogeneity as a mixture of capture probabilities for each individual, and estimates the probability of capture, p_x , for each mixture and the mixture proportion, pi_x . In this analysis the number of mixtures was limited to two, in order to minimize the number of parameters in the model. Rather than select a single model as the best or most confident estimator (i.e., the most parsimonious model with the lowest AIC_c value), we generated a weighted average for the abundance estimate among all models, using the normalized Akaike weights (AIC_c Weights) generated by the MARK selection procedure. Unconditional standard errors and confidence intervals were reported for the weighted average estimates.

Errors in genotyping result in “false negatives” or the same individual sampled twice but assigned different genotypes. Genotyping error is a typical characteristic of large samples of individuals typed for many microsatellite loci, and it is important to assess error and resultant effect on parameter estimation (Waits and Leberg 2000, Lukacs and Burnham 2005). If false negatives occurred between years the result would be that some recaptures are missed and m is under represented. In a dataset such as this with a small probability of capture and sparse recaptures, missing even 1 or 2 recaptures will have substantial positive bias on the abundance estimate. If it occurred within a year, the result would be an inflation of the sample size for the year, also resulting in a positive bias on abundance estimation. Waits and Leberg (2000) used simulations to assess potential magnitude of bias, and concluded that a positive bias could be >200% when using 7-10 loci with an average error of 0.05/locus. This drops substantially (e.g., <20%) when error is decreased to 0.01 or 0.005/locus. Program MARK incorporates a set of closed population models that allow for estimates of misidentification of marks, in this case attributable to genotypic error (based on the models of Lukacs and Burnham 2005). For each closed model there are two additional parameters, alpha, α , the probability that a genotype is correct ($1 - \text{genotypic error probability}$), and f_0 , the number of individuals never captured, whereas abundance, N , is estimated as a derived parameter. We ran all model variations fixing α at 1.0 (no genotyping errors and therefore no misidentifications) and using the observed and predicted genotypic error rate to assess the effect of error on abundance estimation. For estimation of abundance we ran only the models that fixed α , thus incorporating genotyping error, and generated a weighted average for the derived parameter, N , as described above. Genotypes were run both as a sex-aggregated dataset (males and females) and a male-limited dataset. The latter was to address potential heterogeneity as introduced by females potentially having a lower capture probability.

During the intersessional meeting on Southern Hemisphere Humpback Whale Assessment Methodology in January 2009, the working group recommended the application of an open population model, the Pradel model which parameterizes recruitment, survival and population growth (IWC 2009, SC/61/Rep8). We used the form of the Pradel model that estimates the parameters Phi, ϕ , survival and Lambda, λ , the realized growth rate. Models were constructed with various combinations of parameter estimation; in each model p varied by sample occasion (t), and Phi and Lambda was either estimated as a constant, or fixed at values bracketing realistic expectations ($\phi = 0.95, 0.98$; $\lambda = 1.06, 1.10$). The derived abundance (N) was calculated by dividing capture probability into the sample size for each year (n_i/p_i). The Pradel model was run only for the Photo-ID data since it was not formulated to allow misidentification of marks (genotypic error). In order to estimate abundance we generated a weighted average for p_i , as described above, and used yearly sample sizes, n_i , to estimate abundance.

RESULTS

Photographic Recaptures. Within-year sample size of captured individuals varied for tail flukes photographs (all qualities better than “not useable”) from a low of 24 in 2002 to a high of 184 in 2001. The distribution of photographic identifications varied by date across each season (Fig. 2). Periods of few or no collected identifications resulted primarily from poor weather, however was also influenced by variation in the density of whales. The sample of identifications is particularly small in 2002 due to a limited season of 20 days during which photographs were collected on 12 days. Season duration in all other years ranged from 52 to 66 days with photograph effort ranging from 28 to 37 days (Table 1). Within-year recapture rate ranged from 6% to 18% of individuals captured on more than one day. Recaptured individuals had short “residency” intervals between first and last capture with a mean ranging from 3 to 8 days and median values of 2 days for all years except 2002, the anomalous sampling year.

A total of 33 individuals were captured in multiple years, accounting for 44 pair-wise recapture events when using data of all qualities. Between 2000 and 2004 (2005 and 2006 data yet to be examined), yearly

timing of first capture day for recaptured individuals displayed remarkable consistency, with the majority of recaptured individuals being seen on similar dates in different years (Table 2, Fig. 3). In 21 cases, 16 (76%) were recaptured within 10 Julian days of the date of their initial year's capture, 13 (62%) within 5 days, and 7 (33%) within 2 days. To assess the probability of these data in a random distribution, a simple permutation routine was written. For each year, the first date of capture for each individual was randomly permuted among individuals captured that year, and the mean difference in Julian days between recapture dates was calculated for all pair-wise events. The use of the actual data structure (i.e., capture dates) controls for variation and inconsistencies in data collection effort between years. After 10,000 iterations a random distribution was constructed of both the actual individual pair-wise differences in Julian day of capture (Fig. 3), and the mean difference in Julian days across the 21 recapture events. The random mean was 23.26 Julian days (s.d. 15.98). The observed mean of 6.76 Julian days (s.d. 6.64) had a $p < 0.0001$ in the randomly generated distribution (e.g., in 10,000 iterations, there were no runs that had a mean equal to or less than the observed mean).

After eliminating poor quality and partial flukes for use in capture-recapture parameter estimation, the sample of individuals was reduced to a low of 16 individuals in 2002, and between 89 and 159 individuals for the remaining years (Table 3). Recaptures between pairs of years were sparse, ranging from 0 to a maximum of 4. In 2006 a total of 9 of 158 individuals (5.7%) had been seen in any previous year. Of 812 individuals identified across the five years, 28 (3.4%) were captured in more than one year, with one individual captured in a maximum of four different years, and three individuals captured in three different years. Limiting recapture data by quality resulted in the elimination of four recaptures of poor quality or partial flukes.

Genetic Recaptures. A total of 1126 biopsies collected between 2000 and 2006 in Antongil Bay were analyzed. Yearly sample size ranged from 35 to 208 during 2000-2006 (Table 4). Based on genotype identity ($PI=5.6 \times 10^{-12}$), the samples were assigned to 922 unique individuals. Thirty-nine individuals (4.2%) were encountered in multiple years for a total of 47 recaptures between pairs of years. For individual pairs of samples with matching genotypes, GP ranged from 7.0×10^{-17} to 2×10^{-9} , therefore there is strong support for the assumption that the samples came from the same individuals. The yearly sample sizes of individuals ranged from 28 to 185 with a resample rate of 11.1% to 20.8% (Table 4) and the number of recaptures between each pair of years ranged from 0 to 6 (Table 5).

Replication of 182 samples (16.2%) revealed 13 samples that had at least one allelic mismatch in at least one locus, yielding an observed error per genotype of 7.14%. As some genotypes had more than one locus and allelic mismatch, there were a total of 18 single-locus mismatches and 22 allelic mismatches for a mean allelic error rate of 0.6%. Locus-specific error rates ranged from 0.55% (1 mismatch) to 2.75% (5 mismatches). Three loci had no observed mismatches, and error was estimated at 10% of the minimum observable (one mismatch), or 0.055%. Mean error per locus was 1.01%. In order to generate the predicted genotype error rate based upon locus-specific error, we need to calculate the probability that a genotype is correct; that is, simultaneously correct for all loci, or the product of 1-error for all loci. The probability for a genotype to be correct in this dataset was 0.9035, and thus the predicted error rate per genotype was 9.65%. For the purposes of abundance estimation both the observed error rate (7.14%) and the predicted error rate (9.65%) were used to bracket minimum and maximum genotypic error in the dataset.

Photographic Closed Model Abundance Estimates. Considering first estimates derived from flukes photographs, pair-wise Chapman's estimates from consecutive years ranged from 539 (CV=0.39) for years 2002-2003, to 6434 (CV=0.49) for years 2003-2004 (Table 6). Both estimates involving 2002 were anomalously small, and considered unreliable due to the small sample size of 2002 photographs, as well as biased due to timing characteristics of individual recaptures (see discussion below). There was no apparent increasing trend in the magnitude of the point estimates, with the estimates for years 2005 and

2006 being smaller than those for 2003 and 2004 (the highest as noted above). CV's were generally large, close to 0.40 or higher, and thus confidence intervals were large and broadly overlapping.

The poorly represented 2002 sample year was removed for multiple sample closed model estimation. In order to limit the positive bias introduced by closure violation, the samples were split into two non-overlapping, temporally consecutive spans of years, and models were run for 2000-2003 and 2004-2006 data (Table 7). The AIC selection procedure indicated 97.5% support for Model M_t in the 2000-2003 (see Appendix I), therefore this model was predominant in the Weighted Average estimate of 5564. Support in the 2004-2006 dataset was split nearly evenly between Model M_0 and M_h , which together accounted for 90.1% of support, with only 8.7% attributed to M_t . Thus with Weighted Average estimate of 7406 is intermediate between the estimates of M_0 and M_h , the latter pulling the point estimate up. There is a clear increasing trend between two datasets that allows the estimation of an apparent annual rate of increase (ROI) during the three year interval. The ROI value of 0.100 estimated from the Photo-ID data is at the limit of reasonable population growth. This is likely higher than the actual population growth due to the outcome of the selection procedure, and the fact that only the later estimate substantially incorporates M_h , compensating for heterogeneity.

Genotypic Closed Model Abundance Estimates. In order to assess the potential effect of genotyping error on abundance estimation, we ran all closed models on the genotypic recapture data fixing α at 1.00 (no error), 0.9286 (observed error rate per genotype of 0.0714) and 0.9035 (predicted probability of error per genotype of 0.1005). There was a clear trend of reduction in the abundance estimate that was very similar for all models, and the results of Model M_0 using the 2004-2006 dataset is reported to illustrate the effect (Table 8). The estimate without accounting for error of 8312 is reduced substantially when genotype error is incorporated. Assuming that error is a real characteristic of the dataset and the models that fix $\alpha < 1.0$ are more accurate, then the positive bias associated with the non-corrected estimate is 15.9% when considering the smaller observed genotypic error rate, and 23.4% when considering the larger predicted genotypic error rate. This assessment of bias is congruent with that reported by Waits and Leberg (2000) for the general level of error measured in this analysis. Assuming that the true probability for mismatches is somewhere between the observed and predicted genotypic error rates, all closed models were run for each value of α .

The sex-aggregated genotypic data (both males and females) were run for both three-year datasets as described above. For the 2000-2003 dataset, the two runs for Model M_t had near identical weights and accounted for 95.6% of support (see Appendix II). Thus the Weighted Average estimate of 4836 was largely the mean between the two models bracketing the different error rates (Table 9). For the 2004-2006 dataset, 77.8% of support was attributed to the two M_0 models, whereas 11.5% and 10.4% were attributed to the M_t and M_h models, respectively. For each pair, the models with the different α had near identical weights. The parameter estimation results of the three different assumption models (M_0 , M_t and M_h) were very similar, so the Weighted Average estimate of 6981 is again largely the mean between the models bracketing the different error rates. The apparent ROI of 0.130 is high and unrealistic, indicating some potential inaccuracy in one or both of the 3-year datasets.

It is worthwhile noting that the sex-aggregated genotypic averaged estimates are similar and somewhat smaller than the estimates for the photo-ID data, most notably with only a 5.7% difference in the 2004-2006 model. Thus the application of the genotypic error rate to the genotype recapture models has resolved the conflict between the datasets reported in Cerchio et al. (2008; SC/61/SH32), in which the genotypic estimate was 23.9% larger than the photo-ID estimate for the 2004-2006 datasets. Genotypic error resulting in mis-identifications was one postulated cause for the discrepancy, and as demonstrated the estimated error in this genotypic data is congruent with the observed discrepancy.

Next the genotypic data was restricted to males, to assess the possibility of heterogeneity introduced by a lower capture probability of females. For the 2000-2003 dataset, the two runs for Model M_t had identical weights and accounted for 71.0% of support, whereas the runs for Model M_{th} had near identical weights and accounted for 28.8% of support (see Appendix II). The weighted average estimate of males in the populations was 2780; assuming sexual parity the population abundance estimate is thus 5560. For the 2004-2006 dataset, 78.1% of support was attributed to the two M_0 models, whereas 11.2% and 10.4% were attributed to the M_t and M_h models, respectively (similar to the sex-aggregated results). The weighted average estimate of males for 2004-2006 in the populations was 4163; assuming sexual parity the population abundance estimate is thus 8325. As with the sex-aggregated estimates, the apparent ROI of 0.144 is high and unrealistic, indicating some potential inaccuracy in one or both of the 3-year datasets. The population wide estimates derived from the male data are larger than the sex-aggregated estimates by 15.0% for 2000-2003, and 19.3% for 2004-2006, suggesting there may be some heterogeneity introduced by female behavior and resultant capture probability, or alternatively, the population is not at sexual parity, and may be male biased.

Photographic Open Model Pradel Abundance Estimates. The Pradel model was applied to only the Photo-ID dataset, because the model does not incorporate a parameter for mis-identifications and it has been demonstrated that genotypic error is likely inflating the non-corrected estimates in the Genotypic closed models. The Pradel model that parameterizes survival (ϕ) and growth rate (λ) was initially run to estimate ϕ and λ as constants, and p_i varying by year. This initial run yielded an estimate of ϕ of 0.746 that was unrealistically small, and an estimate of λ of 1.069 that was within expectation (see Appendix III, Model $\phi(.)\lambda(.)p(t)$). Estimates of p_i were large relative to other models run, ranging from 0.027 to 0.045 and consequently yielded relatively small estimates of abundance; support for the model was intermediate at 16.0% (Appendix III). Therefore, the intersessional working group (IWC 2009, SC/61/Rep8) recommended that we next fix ϕ , bracketing reasonable expectations of 0.95 and 0.98 (Appendix III, models $\phi(.95)\lambda(.)p(t)$ and $\phi(.98)\lambda(.)p(t)$, respectively); this yielded unrealistically high estimates of λ of 1.146 and 1.159, respectively, and consequently the largest estimates of all models. Support for these models was the lowest of all in the Pradel set of runs, at 8.9% and 5.6%, and consequently contributed the least to the weighted average. We then fixed λ , bracketing reasonable expectations of 1.06 and 1.10 to run with both fixed values of ϕ . Models $\phi(.95)\lambda(1.10)p(t)$ and $\phi(.95)\lambda(1.06)p(t)$ had the most support among all models, which were similar at 23.2% and 20.0%, respectively (Appendix III). These models consequently had the most influence in the final weighted average estimates. Models $\phi(.98)\lambda(1.10)p(t)$ and $\phi(.98)\lambda(1.06)p(t)$ had low to intermediate support, at 14.2% and 11.9%, respectively, but together contributed a full quarter of the input to the weighted average estimates.

The Weighted Average estimates of p_i among all Pradel models ranged from 0.0181 to 0.0296 and yielded steadily increasing abundance estimates from 5370, in 2000, to 8169, in 2006 (Table 11). Precision was the lowest among all models, with CVs ranging from 0.38 to 0.51, and consequently 95% confidence intervals were large. The effective growth rate for the weighted average was approximately 1.09 (ranging from 1.0900 in 2000-2001 to 1.0859 in 2005-2006); however, since four of the seven models averaged had this parameter fixed at either 1.06 or 1.10, this should not be considered an estimate of the parameter.

DISCUSSION

There are several considerations to keep in mind when evaluating these abundance estimates. *The primary concerns effecting accuracy are heterogeneity of capture probability introduced by the consistent timing of capture of individuals, the small sample size relative to population size (low probability of capture), the potential for bias due to closure violations in the closed capture models, and the fit of the data to the Pradel model.* We must also consider the extent of the region which these

estimates represent. Specifically, the sampling from one site is likely not representative of the geographic and within season movements of the entire population that is likely to be frequenting Madagascar.

Heterogeneity, Precision and Accuracy of Estimates

An important aspect of this dataset is the strong consistency observed in Julian date recaptures of individuals between years. This has significant ramifications for sampling design on the resultant estimate bias. On one extreme, sampling during the same short period each season would introduce heterogeneity and negative bias, since those animals that have a tendency to arrive during the period of sampling would have a much higher probability of capture than others. Conversely, sampling during short periods at different non-overlapping times of the season could result in significant positive bias due to sampling essentially different sub-populations. ***It is therefore clearly important to sample throughout the season and during the same periods each year, or otherwise there is a high risk of sampling different portions of the population moving through the sampling site at different times.*** This clearly has important implications for both mark-recapture as well as genetic studies looking at population structure across broad regions.

In our study, this issue calls into question the use of yearly samples that are not completely concurrent, such as the highly abbreviated 2002 photographic sample. The anomalous estimates that are derived from these samples when using them in pair-wise Chapman's estimate corroborate this conclusion, as does the observation that when the 2002 photographic data is removed, the respective estimates increase. To further explore this effect, we generated a set of estimates using photographic data that was constrained to the brief period of sampling in 2002 between Julian days 230 and 255 using the Chapman's Modified Petersen (Table 12). Estimates were in all cases lower than those for the same models and years when using all data, indicating significant heterogeneity when restricting the data to the truncated sample period. In the most extreme case, the pair-wise estimate for 2000-2001 was nearly tenfold smaller. For this reason we excluded the 2002 sampling year from all subsequent estimation models.

Due to the relatively small yearly sample sizes for the apparent size of this population (i.e., low capture probabilities), the observed number of recaptures were small and resulted in poor precision. This is particularly true with the pair-wise Chapman's estimates, with CV's ranging from ca 0.30 to 0.49. Precision was somewhat improved in the closed model multiple year estimates, ranging from a CV of 0.33 to 0.39. Precision was also poor among the Pradel model estimates ranging from 0.38 to 0.51, likely due to increase in the number of estimated parameters for the open model. Furthermore, the use of model averaging and unconditional standard error also contributes to lower precision. ***Thus, due to the poor precision resulting from the limitations of the dataset, we strongly suggest caution when applying any of these estimates to population assessment and management decisions.***

Use of closed population models is generally not advised over multiple years due to a positive bias associated with violations of closure. In this analysis we attempted to limit this bias by limiting the number of sample years in the MARK closed models to three years. There is likely still some bias associated with these estimates, and they are in most cases larger than consecutive year Chapman estimates. This trend (larger three-year estimates) may also reflect the presence of heterogeneity (negative bias) in the simple two-year Chapman estimates, which the MARK models compensate for both by inclusion of more sample years and relaxation of model assumptions (i.e., influence of Model M_h in at least the 2004-2006 photographic data weighted average estimate).

The Pradel open model was used since this population is clearly not closed, particularly over the seven sample years, and it allows the use of all available data. The Pradel model is formulated to estimate survival, realized population growth and capture probability, the latter of which is secondarily used to estimate abundance. With all parameters unconstrained, the estimated survival rate was unrealistically low at 0.75, reflecting a poor fit of the data to the model. Alternatively, this could indicate the presence

of emigration from the population; in such a case it should be considered that the low 2006 estimate of 4936 (2137, 11692) (Appendix III) may represent a core population in C3 that preferentially migrates to Antongil Bay. Thus by constraining survival to larger realistic values we may be forcing the model to estimate some larger global population (see *Geographic implications* discussion below). Furthermore, fixing survival between 0.95 and 0.98 results in an unrealistically high growth rate, which in turn must be fixed to force the model to generate capture probabilities that are considered reasonable. ***The utility of a model should be reviewed, given that two of the three parameters it is designed to estimate need to be fixed in order to produce an acceptable estimate for the third. The resultant accuracy of the results may therefore be suspect and should be evaluated by the members of the sub-committee.***

RECOMMENDATIONS

Given these caveats, for the purposes of the comprehensive assessment we recommend the following. We suggest use of two estimates for current abundance in 2006, bracketing a lower-bound and an upper-bound. As a lower bound estimate for the larger population, we recommend the genotypic data, closed model, sex-aggregated weighted average estimate of 6981, CV=0.33, 95% confidence interval of 2525-11437. Alternatively, as a more conservative lower bound estimate, potentially representing at least the east coast of Madagascar (see discussion below), we recommend the Pradel unconstrained model estimate of 4936, CV=0.44, 95% confidence interval of 2137-11692. As an upper bound estimate, we recommend the Pradel model, photographic data of 8169, CV=0.44, 95% confidence interval of 3476-19497.

Geographic implications

Lastly, we must consider the question of exactly what group of whales we are estimating the abundance for. These samples were collected in one restricted area, Antongil Bay, within the C3 breeding sub-region off Madagascar. There are several levels in which we need to evaluate what this sample represents: Antongil Bay relative to sub-region C3; sub-region C3 relative to all of region C; and region C relative to other breeding regions, particularly B and D.

Within Madagascar. We have little data from other areas around Madagascar, therefore attributing these estimates to C3 in general makes an assumption regarding mixing of animals around Madagascar. There are observations and reports of concentrations of humpback whales further south on the east coast (e.g., Ile St. Marie, Ft. Dauphin) as well as along the west coast from Toliara north to Nosy Be (Best et al. 1997, Cerchio, Razafindrakoto and Rosenbaum unpub. data, Findlay pers. comm.). Further research is required to determine how these whales mix, particularly those off the west relative to the east coasts. Given the general mobility of humpbacks whales in other regions (e.g. among the Hawaiian Islands, Cerchio et al 1998), the short apparent residency time in Antongil Bay (Table 2), and data indicating longer-distance movements between C3 and C2 (Ersts et al. 2006) as well as between C3 and C1 (Pomilla 2005, Pomilla et al 2006), we find it reasonable to assume these estimates at least represents the C3 sub-region specifically.

Within the West Indian Ocean. Regarding the relationship of the three currently designated sub-regions within region C, there is emerging evidence suggesting differential exchange. Genetic analyses have indicated significant differentiation between C3 and C1 for both mtDNA (Rosenbaum et al. 2006) and nDNA microsatellites (Pomilla 2005, Pomilla et al. 2006). However, the same analyses indicated no differentiation between C3 and C2. Recapture of individuals (from both photographic and genetic data) indicate exchange of individuals, potentially significant, between C3 and C2 (Ersts et al. 2006). Further work and larger samples from C2 are required to test whether there is random exchange and panmixis between individuals from C2 and C3. However, our current understanding suggests the possibility, if not likelihood, that these sub-regions are contiguous and our estimate may reflect abundance for both C2 and C3.

Regarding C3 and C1, although population genetic analyses reveal significant differentiation, it is not as great as between C3 and equivalently sampled sub-regions in region B or D (Pomilla 2005, Rosenbaum et al. 2006; Pomilla et al. 2006, Rosenbaum et al. 2006). Furthermore we have reported a genetic recapture between C3, Antongil Bay, and C1, East South Africa (Pomilla 2005, Pomilla et al. 2006), and two photographic recaptures also between Antongil Bay and East South Africa (Cerchio et al. 2008, SC/60/SH33). These localities in C1 are thought to be predominately a migration corridor in the southern range of C1, and thus might represent a stream of animals migrating to breeding areas in northern C1 as well as C2/C3. The results of the photographic comparison between (southern) C1 and C3 suggested that these groups are not randomly associating, because the probability of recapture between the areas was significantly less than the probability of recapture within the areas (Cerchio et al. 2008, SC/60/SH33). However, there is clearly some exchange and the photographic sample from C1 was too temporally and geographically inconsistent, and recaptures too sparse to draw definitive conclusions regarding degree of exchange; thus an index of mixing was not reported or advised (Cerchio et al. 2008, SC/60/SH33). There is very little data from Mozambique and other areas of known breeding aggregations in northern C1, so it is as yet impossible to comment on the relationship between these breeding assemblages. Therefore, we conclude that there is likely sufficient exchange between these sub-regions to caution against the simple addition of independent estimates from C3 and C1 to arrive at a region-wide estimate for C. Further characterization of migratory movements and exchange among the sub-regions of C are necessary before we can satisfactorily assess the impact of exchange rates and patterns on estimation of abundance. Given the genetic and observational data combined and the uncertainty regarding population structure in this region, it is ultimately difficult to provide a precise characterization of this estimate as representing C3 with some 'known' degree of mixing between C1 and C3. Based on the evidence available, we recommend revisiting the models for stock structure that were initially drafted at the SH humpback whale workshop in 2006 (Rep 5, JCRM 2007)

Between Indian and Atlantic Oceans. Finally, the relationship between regions B, C and D needs to be more clearly defined to assess the degree of exchange between regions. Our current evidence regarding regions B and C indicate significant differentiation at a level greater than between sub-regions within either region (Pomilla 2005, Pomilla et al. 2006, Rosenbaum et al. 2006). However, there are also two documented movements between Gabon, B1, and Madagascar, C3, detected with genotypic recapture and confirmed with dorsal fin photographs (Pomilla and Rosenbaum 2005, Loo and Pomilla pers. comm.). Movements of whales from breeding grounds (and sub-regions) mediated through adjacent feeding grounds has also been recently detected (Loo et al. 2008). Moreover, recent acoustic analysis indicates that whales from these two regions sing very similar songs sharing all major phrase types (Razafindrakoto et al. 2009, this meeting SC/61/SH8) indicating a cultural exchange that requires a non-trivial exchange of individuals. Little is known about the relationship of Breeding Stocks C and D beyond significant genetic differentiation at mtDNA (Rosenbaum et al. 2006), however there is recent evidence of shared song content and therefore acoustic cultural exchange, although minor in comparison to the B-C similarities (Murray 2007, Murray et al. 2009, this meeting SC/61/SH9).

In summary, we have generated the most current estimates and extensive evaluation of humpback whale population abundance for the C3 breeding region in the southwestern Indian Ocean. Sample size limitations resulted in relatively low precision, and characteristics of individual behavior may introduce bias. However, relative consistency among a variety of models and sample combinations suggests that this population is likely approximately 7000-8000 individuals, however the geographic region to which this population estimate applies needs to be carefully considered and better defined.

ACKNOWLEDGEMENTS

We are grateful to the staff of the WCS/AMNH New York Staff and WCS Country Programs of Madagascar, in particular George Amato, Rob DeSalle, Eleanor Sterling, Helen Crowley and Matthew

Hatchwell, and all the summer interns, students, volunteers and research assistants who have contributed to field and laboratory work, in particular Carla Freitas and Vanessa Rasoamampianina. Many other individuals were involved and helped throughout the years of this study from the WCS Madagascar Country Program, WCS Marine Program, AMNH Center for Biodiversity and Conservation and AMNH Conservation Genetics Program. Funding for this work was provided from grants and awards to WCS and AMNH.

LITERATURE CITED

- Ayres KL, Overall DJ (2004) api-calc 1.0: a computer program for calculating the average probability of identity allowing for substructure, inbreeding and the presence of close relatives. *Molecular Ecology Notes*, **4**, 315-318.
- Begon M (1979) Investigating animal abundance: capture-recapture for biologists. University Park Press, Baltimore.
- Best PB, Findlay KP, Sekiguchi K, *et al.* (1998) Winter distribution and possible migration routes of humpback whales (*Megaptera novaeangliae*) in the southwest Indian Ocean. *Marine Ecology Progress Series*, **162**, 287-299.
- Best PB, Sekiguchi K, Rakotonirina BP, Rossouw A (1997) The distribution and abundance of humpback whales off southwest Madagascar, August-September. *Report to the International Whaling Commission*, **46**, 323.
- Burnham K, Anderson, D (2002) *Model Selection and Multi-Model Inference* (2nd Ed.) Springer-Verlag. 496 pp.
- Cerchio S, Gabriele C, Norris T, Herman LM (1998) Movements of humpback whales between Kauai and Hawaii: implications for population structure and abundance estimation in the Hawaiian Islands. *Marine Ecology Progress Series* **175**: 13-22.
- Clapham PJ, Palsbøll PJ (1997) Molecular analysis of paternity shows promiscuous mating in female humpback whales. *Proceedings of the Royal Society of London - series B*, **264**, 95-98.
- Ersts P, Pomilla C, Rosenbaum HC, Kiszka J, Vely M (2006) Humpback whales identified in the territorial waters of Mayotte [C2] and matches to eastern Madagascar [C3], p. 5. Paper SC/A06/HW12 presented to the IWC, Intersessional Workshop for the Comprehensive Assessment of Southern Hemisphere humpback whales (unpublished).
- Hammond, PS (1986) Estimating the size of naturally marked whale populations using capture-recapture techniques. *Report to the International Whaling Commission, Spec Issue No 8*: 253-282.
- IWC. 2009. Report on the Intersessional Workshop on Southern Hemisphere Humpback Whale Assessment Methodology. Report SC/61/Rep8 presented to the IWC Scientific Committee.
- Lambertsen RH (1987) A biopsy system for large whales and its use for cytogenetics. *Journal of Mammalogy*, **68**, 443-445.
- Lukaes PM and Burnham KP. 2005. Estimating population size from DNA-based closed capture–recapture data incorporating genotyping error. *Journal of Wildlife Management* **69**:396–403

- Murray, A. (2007) *A Characterization and Comparison of Humpback Whale (Megaptera novaeangliae) Song from the Southern Indian Ocean*. M.A. thesis. Columbia University, New York.
- Murray A, Cerchio S, Jenner C, McCauley R, Razafindrakoto Y, McKay S, Coughran D and Rosenbaum H. 2009. Comparison of humpback whale songs in the southern Indian Ocean indicate limited exchange between populations wintering off Madagascar and Western Australia. Report SC/61/SH9 presented to the IWC Scientific Committee.
- Otis DL, Burnham KP, White GC, Anderson R (1978) Statistical inference for capture data closed animal populations. *Wildlife Monographs* **62**: 1-135.
- Palsbøll PJ, Allen J, Bérubé M, *et al.* (1997a) Genetic tagging of humpback whales. *Nature*, **388**, 767-769.
- Pomilla C. (2005) Genetic structure of humpback whale populations on the Southern Hemisphere wintering grounds. PhD Dissertation. New York University.
- Pomilla C, Rosenbaum HC (2006). Estimates of relatedness in groups of humpback whales on two wintering grounds of the Southern Hemisphere. *Molecular Ecology*, **15**, 2541-2555.
- Pomilla C, Rosenbaum HC (2005) Against the current: an inter-oceanic whale migration event. *Biology Letters*, **1**, 476-479.
- Pomilla C. *et al.* (2006) MtDNA diversity and population structure of humpback whales from their wintering areas in the Indian and South Atlantic Ocean (Breeding regions A, B, C and X), p. 12. Paper SC/A06/HW41 presented to the IWC, Intersessional Workshop for the Comprehensive Assessment of Southern Hemisphere humpback whales.
- Razafindrakoto, Y., Cerchio, S., Collins, T., Rosenbaum, H., Ngouesso, S. (2009) Similarity of humpback whale song from Madagascar and Gabon indicates significant contact between South Atlantic and southwest Indian Ocean populations. Report SC/61/SH8 presented to the IWC Scientific Committee.
- Rosenbaum HC, Razafindrakoto Y, Ersts P, Ventresca G. (2000) A preliminary population estimate for humpback whales from the Antongil Bay, Madagascar wintering grounds in the southwestern Indian Ocean. Paper SC/52/IA10 presented to the IWC Scientific Committee, (unpublished).
- Rosenbaum HC, Walsh PD, Razafindrakoto Y, Vely M, DeSalle R (1997) First description of a humpback whale breeding ground in Baie d'Antongil, Madagascar. *Conservation Biology* **11**: 312-314.
- Rosenbaum HC, Pomilla C, Leslie M, *et al.* (2006) Population structure and sex biased gene flow of humpback whales from their wintering areas in the Indian and South Atlantic Ocean (Breeding regions A, B, C and X) based on nuclear microsatellite variation. p. 12. Paper SC/A06/HW38. presented to the IWC, Intersessional Workshop for the Comprehensive Assessment of Southern Hemisphere humpback whales.
- Waits JL, Luikart G, Taberlet P (2001) Estimating the probability of identity among genotypes in natural populations: cautions and guidelines. *Molecular Ecology*, **10**, 249-256.

Waits, JL Leberg, PL (2000) Biases associated with population estimation using molecular tagging. *Animal Conservation*, **3**, 191-199.

White GC, Burnham, KP (1999) Program MARK: Survival estimation from populations of marked animals. *Bird Study* 46 Supplement, 120-138.

TABLES AND FIGURES

Table 1. Within year effort by year in Antongil Bay, Madagascar, for photographic data.

	2000	2001	2002	2003	2004	2005	2006
Yearly Effort							
Start Date	17 July	10 July	22 Aug	11 July	10 July	13 July	16 July
End Date	17 Sept	14 Sept	11 Sept	9 Sept	5 Sept	5 Sept	4 Sept
Duration	62	66	20	60	59	56	52
Sample Days	37	35	12	34	34	28	37

Table 2. Date of first capture for between-year photographic recaptures in Antongil Bay, Madagascar, indicates strong consistency in timing of arrival. Of 21 recapture events between years (comprised of 19 individuals), 7 (33%) were sighted within two days of their first sighting date, 13 (62%) within five days, and a total of 16 (76%) within ten days.

Individual	2000	2001	2002	2003	2004	Difference in Julian Days ¹
TF-MAD-00-008	7/22/2000				7/20/2004	2
TF-MAD-00-019	8/7/2000			8/26/2003		18
TF-MAD-00-031	8/27/2000				8/14/2004	13
TF-MAD-00-041	9/7/2000			9/7/2003		1
TF-MAD-00-081	7/29/2000			7/29/2003		1
TF-MAD-00-095	9/2/2000	9/9/2001	9/4/2002			6,1,5
TF-MAD-00-098	9/8/2000	9/6/2001				3
TF-MAD-01-041		7/27/2001			7/19/2004	7
TF-MAD-01-077		8/19/2001		8/18/2003		1
TF-MAD-01-139		7/18/2001			7/21/2004	4
TF-MAD-01-189		8/7/2001			8/5/2004	1
TF-MAD-01-194		9/6/2001		8/16/2003		21
TF-MAD-02-001			8/28/2002	8/24/2003		4
TF-MAD-02-003			9/2/2002	8/26/2003		7
TF-MAD-02-010			9/4/2002	8/17/2003		18
TF-MAD-02-021			9/6/2002	9/7/2003		1
TF-MAD-03-037				7/28/2003	8/14/2004	18
TF-MAD-03-118				7/12/2003	7/16/2004	5
TF-MAD-03-140				7/19/2003	7/13/2004	5

¹Julian Day is calculated using 1 January as "1"; leap years in 2000 and 2004 with 366 days account for the apparent inconsistencies between differences in calendar dates and Julian days.

Table 3. Yearly sample sizes and recaptures for tail flukes in Antongil Bay, Madagascar.

	2000	2001	2002	2003	2004	2005	2006
Individuals captured	89	159	16	126	151	144	158

Year of Initial Capture	Year of Recapture						
	2000	2001	2002	2003	2004	2005	2006
2000	X	2	1	3	1	0	1
2001		x	1	3	3	3	2
2002			x	3	0	0	0
2003				x	2	1	3
2004					x	4	3
2005						x	4
2006							x

Table 4. Within year sample characteristics by year in Antongil Bay, Madagascar, for genetic data.

	2000	2001	2002	2003	2004	2005	2006	Total
Number samples	142	187	35	208	193	188	173	1126
Number Individuals	114	161	28	185	162	160	154	921
Resample Rate	19.7%	13.9%	20.0%	11.1%	16.1%	14.9%	11.0%	18.2%

Table 5. Yearly sample sizes and recaptures for genotypes in Antongil, Madagascar.

	2000	2001	2002	2003	2004	2005	2006
Individuals captured	114	161	28	185	162	160	154

Year of Initial Capture	Year of Recapture						
	2000	2001	2002	2003	2004	2005	2006
2000	x	4	1	2	2	0	0
2001		x	2	6	2	1	2
2002			x	6	1	1	1
2003				x	2	2	3
2004					x	2	4
2005						x	3
2006							x

Table 6. Abundance estimates using tail flukes photo-IDs and applying Chapman's modified Petersen estimator to pairs of consecutive years.

Photo-IDs					
Years	N	SE	CV	LCL	UCL
2000-2001	4799	2337	0.49	218	9380
2001-2002	1359	733	0.54	0	2796
2002-2003	539	208	0.39	132	946
2001-2003	5079	2208	0.43	752	9406
2003-2004	6434	3148	0.49	264	12603
2004-2005	4407	1739	0.39	999	7815
2005-2006	4610	1820	0.39	1042	8178

Table 7. Closed population capture-recapture model abundance estimates using tail flukes photo-IDs and applying Program MARK. For each dataset several models were run, including: M_0 =the null model; M_t =capture probability varies with sampling occasion; M_h = capture probability varies with individual (heterogeneity); and M_{th} = capture probability varies with sampling occasion and individual. Support for models was determined based upon Akaike's Information Criteria, AIC_c (detailed in Appendix I). Estimates of abundance reported below are the weighted average of all models run based on AIC_c Weights. Individual model results are reported in Appendix I. Two non-overlapping datasets were used each having three sample years, providing estimates for the years 2003 and 2006; these estimates were then used to calculate a cursory rate of increase (ROI) for the population.

Photo-IDs						
Dataset	Model	<i>N</i>	SE	CV	LCL	UCL
2000-2003, excluding 2002	Weighted Average	5564	1999	0.36	1646	9482
2004-2006	Weighted Average	7406	2704	0.37	2106	12706
ROI		0.100				

Table 8. Exploring the effect of genotyping error and probability of misidentification of marks on closed population capture-recapture model abundance estimates using Genotypes, sex-aggregated (both males and females), applying Program MARK. The null model is used to illustrate the biased introduced when genotyping error is not accounted for. Error was independently assessed with 182 replicate processed samples and two error rates used: the observed genotypic error rate, 7.14% (proportion of genotypes with errors at one or more loci) and the predicted genotypic error rate, 10.05% (summation of locus-specific error rates). The α parameter describes the probability that a genotype is without error (1 – error probability). All closed models (M_0 , M_t , M_h , M_{th}) were run with each value of α with similar resulting estimates of bias as shown for M_0 .

Genotypes, Sex-aggregated							
Dataset	Model	α	<i>N</i>	SE	LCI	UCI	Bias in $\alpha=1.0$
2004-2006	M_0	1.000	8312	2701	4468	15466	
2004-2006	M_0	0.9286	7173	2326	3860	13330	15.9%
2004-2006	M_0	0.9035	6734	2181	3626	12506	23.4%

Table 9. Closed population capture-recapture model abundance estimates using Genotypes, sex-aggregated (both males and females), and applying Program MARK. Procedure is as described in Table 7 for Photo-IDs. Each model (M_0 , M_t , M_h , M_{th}) was run allowing for mis-identification of marks with an $\alpha = 0.9286$ and 0.9035 , the observed and predicted genotype error rate. Two non-overlapping datasets were used each having three sample years, providing estimates for the years 2003 and 2006; these estimates were then used to calculate a cursory rate of increase (ROI) for the population.

Genotypes, Sex-aggregated						
Dataset	Model	<i>N</i>	SE	CV	LCL	UCL
2000-2003, excluding 2002	Weighted Average	4836	1562	0.39	1775	7898
2004-2006	Weighted Average	6981	2273	0.33	2525	11437
ROI		0.130				

Table 10. Closed population capture-recapture model abundance estimates using Genotypes, males only, and applying Program MARK. Procedure is as described in Table 7 for Photo-IDs. Each model (M_0 , M_i , M_h , M_{th}) was run allowing for misidentification of marks with an $\alpha = 0.9286$ and 0.9035 , the observed and predicted genotype error rate. Assuming sexual parity in the population, the estimates and confidence limits are doubled to estimate population abundance. Two non-overlapping datasets were used each having three sample years, providing estimates for the years 2003 and 2006; these estimates were then used to calculate a cursory rate of increase (ROI) for the population.

Genotypes, Male-limited							
Dataset	Model	Sex	N	SE	CV	LCL	UCL
2000-2003, excluding 2002	Weighted Average	M	2780	1021	0.37	778	4782
		M+F	5560			1556	9564
2004-2006	Weighted Average	M	4163	1531	0.37	1161	7164
		M+F	8325			2323	14328
ROI			0.144				

Table 11. Pradel open population capture-recapture model results using tail flukes Photo-IDs and applying Program MARK. Several models were run, and in each model p varied by sample occasion (t), and Phi and Lambda were either estimated as a constant (.) or fixed at values bracketing realistic expectations (Phi=0.95, 0.98; Lambda=1.06, 1.10). Detailed results of all models are provided in Appendix III. Reported below are the Weighted Averages of parameter estimates for $p(t)$ across all models, applying the AIC_c Weights, and the derived abundance (N) calculated by dividing capture probability into the sample size for each year (n_t/p_t).

Year	Est. of p_i	SE	CV	LCL	UCL	n	N	LCL	UCL
2000	0.0181	0.0092	0.51	0.0066	0.0483	89	4927	1842	13442
2001	0.0296	0.0132	0.45	0.0122	0.0699	159	5370	2276	12988
2003	0.0198	0.0076	0.38	0.0093	0.0416	126	6365	3025	13551
2004	0.0218	0.0083	0.38	0.0103	0.0456	151	6922	3310	14663
2005	0.0191	0.0077	0.40	0.0087	0.0418	144	7522	3449	16616
2006	0.0193	0.0085	0.44	0.0081	0.0455	158	8169	3476	19497

Table 12. Abundance estimates using tail flukes, exploring the effect of sampling during a short period. Using the abbreviated 2002 field season as a reference, these abundance estimates were generated using only concurrent sampling, thereby truncating the data to only captures made during the 25-day period of Julian day 230 to 255 for all years. In all cases, these estimates are two to ten-fold smaller than when using all data.

	N	CV	95%CI
2000-2001	549	0.46	+/- 498
2001-2002	296	0.53	+/- 307
2002-2003	350	0.53	+/- 365
2003-2004	1754	0.69	+/- 2374

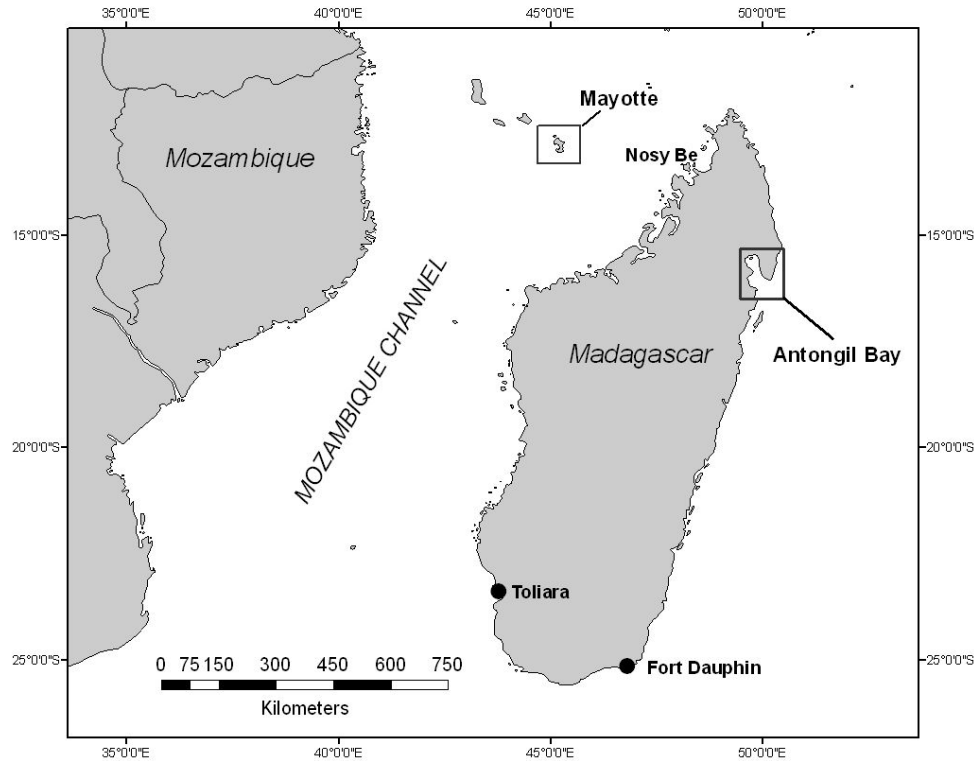


Figure 1. Location of study site, Antongil Bay, Madagascar.

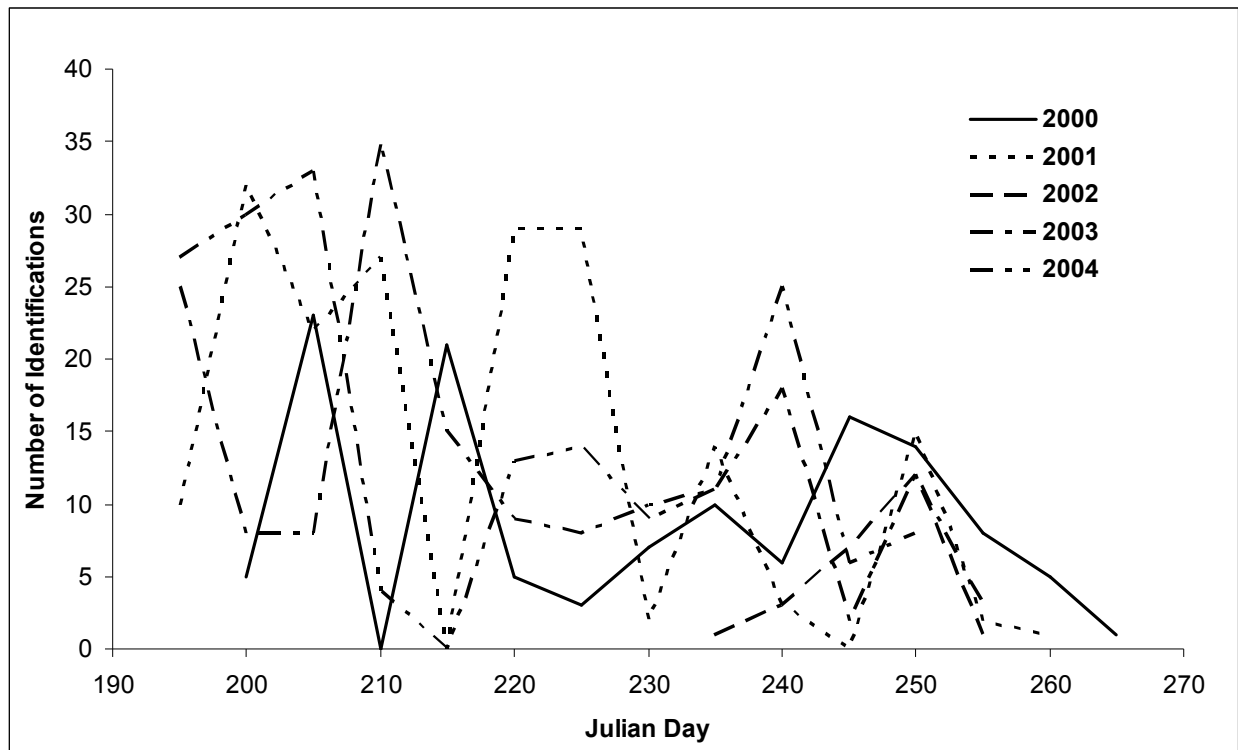


Figure 2. Sampling profile in Antongil Bay, Madagascar, expressed as number of photographic identifications collected in 5-day blocks for 2000 through 2004. Number of IDs collected varied throughout each year primarily due to weather constraints as well as density of whales. The 2002 season (red) was strongly abbreviated due to political upheaval in Madagascar early in the year.

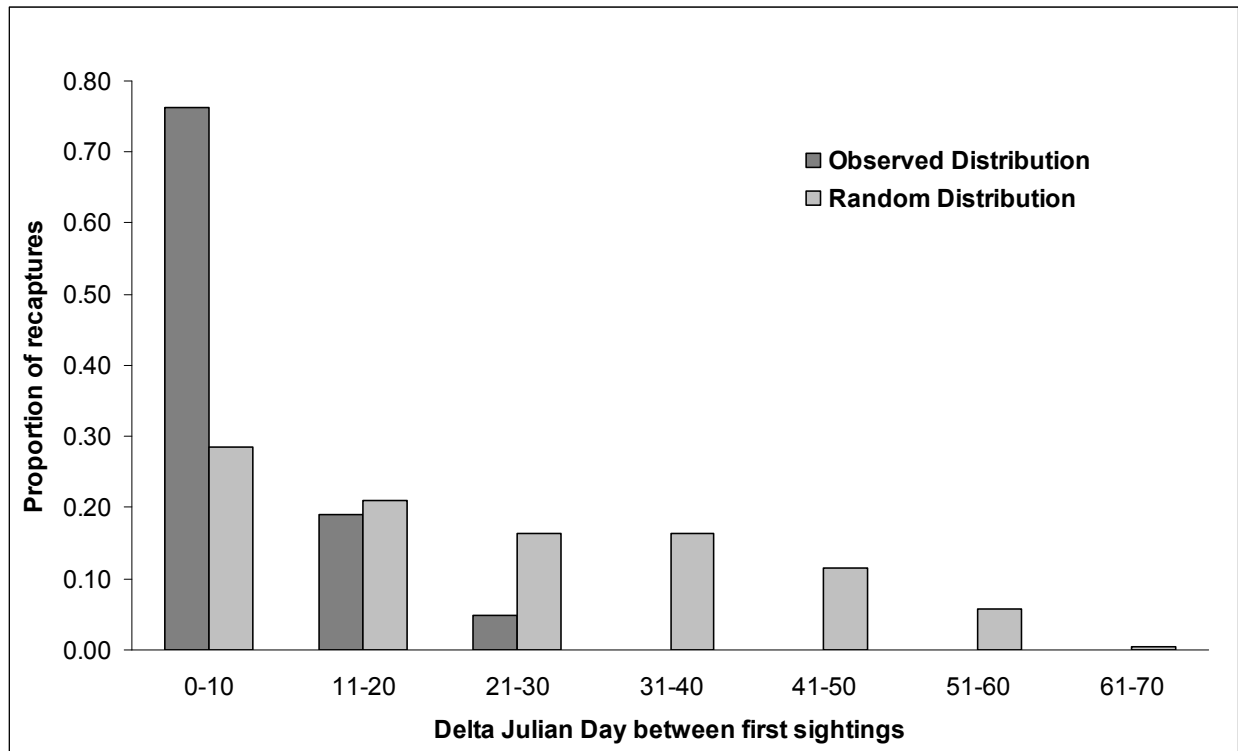


Figure 3. Timing of between-year recaptures in Antongil Bay, Madagascar, indicating highly significant consistency in capture date between years (10,000 permutations, $p < 0.0001$). Random distribution was generated by randomly permuting the capture date of all captured individuals within each year and recalculating the difference in Julian day of capture for each recaptured individual.

APPENDIX I

Photographic Data – Model outputs from Program MARK including AIC results and parameter estimates for abundance (N). Model runs with a Delta AIC_c < 2, indicating strong support, are indicated in **bold** text.

Mad 2000-2003, no 2002

Model	AIC _c	Delta AIC _c	AIC _c Weights	Model Likelihood	Num. Param.	Deviance
Model M_t	-2719.95	0.000	0.97491	1.0000	4	8.466
Model M _{th}	-2712.61	7.344	0.02479	0.0254	8	7.713
Model M _o	-2703.49	16.466	0.00026	0.0003	2	28.957
Model M _h	-2699.46	20.491	0.00003	0.0000	4	28.957

Model	Weight	N	SE	CV	LCL	UCL
Model M_t	0.97491	5612	1925	0.34	2980	10896
Model M _{th}	0.02479	3670	3421	0.93	986	17970
Model M _o	0.00026	5763	1979	0.34	3057	11193
Model M _h	0.00003	5763	1979	0.34	3057	11193

Mad 2004-2006

Model	AIC _c	Delta AIC _c	AIC _c Weights	Model Likelihood	Num. Param.	Deviance
Model M_o	-3429.90	0.000	0.48734	1.0000	2	12.518
Model M_h	-3429.58	0.326	0.41402	0.8496	4	8.823
Model M _t	-3426.46	3.446	0.08702	0.1786	4	11.942
Model M _{th}	-3422.43	7.472	0.01162	0.0238	8	7.890

Model	Weight	N	SE	CV	LCL	UCL
Model M_o	0.48734	6737	2067	0.31	3804	12229
Model M_h	0.41402	8226	2874	0.35	4305	16127
Model M _t	0.08702	6733	2066	0.31	3802	12222
Model M _{th}	0.01162	11279	7925	0.70	3446	39531

APPENDIX II

Genotypic Data– Model outputs from Program MARK including AIC results and parameter estimates for abundance (N). Model runs with a Delta AIC_c < 2, indicating strong support, are indicated in **bold** text.

Mad 2000-2003, excluding 2002, Sex-aggregated

Model	AICc	Delta AICc	AICc Weights	Model Likelihood	Num. Param.	Deviance
M_t α = 0.9286	-3488.866	0.0000	0.48342	1.0000	4	9.3270
M_t α = 0.9035	-3488.861	0.0048	0.48226	0.9976	4	9.3319
M _{th} α = 0.9035	-3482.142	6.7245	0.01675	0.0346	8	7.9736
M _{th} α = 0.9286	-3482.142	6.7245	0.01675	0.0346	8	7.9736
M _o α = 0.9286	-3474.538	14.3278	0.00037	0.0008	2	27.6759
M _o α = 0.9035	-3474.402	14.4643	0.00035	0.0007	2	27.8123
M _h α = 0.9286	-3470.517	18.3488	0.00005	0.0001	4	27.6759
M _h α = 0.9035	-3470.381	18.4853	0.00005	0.0001	4	27.8123

Model	Weight	N	SE	CV	LCL	UCL
M_t α = 0.9286	0.48342	4930	1369	0.28	2890	8410
M_t α = 0.9035	0.48226	4632	1284	0.28	2717	7897
M _{th} α = 0.9035	0.01675	3642	2030	0.56	1314	10095
M _{th} α = 0.9286	0.01675	3900	2583	0.66	1196	12719
M _o α = 0.9286	0.00037	5083	1413	0.28	2978	8675
M _o α = 0.9035	0.00035	4802	1333	0.28	2815	8191
M _h α = 0.9286	0.00005	5083	1413	0.28	2978	8675
M _h α = 0.9035	0.00005	4802	1339	0.28	2808	8210

Mad 2004-2006, Sex-aggregated

Model	AICc	Delta AICc	AICc Weights	Model Likelihood	Num. Param.	Deviance
M_o α = 0.9035	-3687.622	0.0000	0.39003	1.0000	2	9.0122
M_o α = 0.9286	-3687.613	0.0095	0.38818	0.9953	2	9.0217
M _t α = 0.9286	-3683.793	3.8291	0.05749	0.1474	4	8.8212
M _t α = 0.9035	-3683.793	3.8296	0.05748	0.1474	4	8.8217
M _h α = 0.9035	-3683.602	4.0201	0.05226	0.1340	4	9.0122
M _h α = 0.9286	-3683.593	4.0296	0.05201	0.1333	4	9.0217
M _{th} α = 0.9286	-3676.558	11.0645	0.00154	0.0039	8	7.9819
M _{th} α = 0.9035	-3675.718	11.9043	0.00101	0.0026	8	8.8217

Model	Weight	N	SE	CV	LCL	UCL
M_o α = 0.9035	0.39003	6734	2181	0.32	3626	12506
M_o α = 0.9286	0.38818	7173	2326	0.32	3860	13330
M _t α = 0.9286	0.05749	7181	2328	0.32	3864	13344
M _t α = 0.9035	0.05748	6744	2185	0.32	3631	12526
M _h α = 0.9035	0.05226	6734	2181	0.32	3626	12506
M _h α = 0.9286	0.05201	7174	2326	0.32	3860	13330
M _{th} α = 0.9286	0.00154	5310	2517	0.47	2197	12834
M _{th} α = 0.9035	0.00101	6744	2185	0.32	3631	12526

Mad 2000-2003, excluding 2002, Male-limited

Model	AICc	Delta AICc	AICc Weights	Model Likelihood	Num. Param.	Deviance
M_t α = 0.9286	-2183.571	0.0000	0.35552	1.0000	4	13.7381
M_t α = 0.9035	-2183.571	0.0000	0.35552	1.0000	4	13.7381
M_{th} α = 0.9035	-2181.767	1.8039	0.14426	0.4058	8	7.4288
M_{th} α = 0.9286	-2181.762	1.8085	0.14393	0.4048	8	7.4334
M _o α = 0.9286	-2169.743	13.8279	0.00035	0.0010	2	31.5963
M _o α = 0.9035	-2169.632	13.9390	0.00033	0.0009	2	31.7073
M _h α = 0.9286	-2165.713	17.8582	0.00005	0.0001	4	31.5963
M _h α = 0.9035	-2165.602	17.9693	0.00004	0.0001	4	31.7073

Model	Weight	N	SE	CV	LCL	UCL
M_t α = 0.9286	0.35552	3132	1000	0.32	1700	5769
M_t α = 0.9035	0.35552	2942	939	0.32	1599	5416
M_{th} α = 0.9035	0.14426	2039	761	0.37	1005	4138
M_{th} α = 0.9286	0.14393	2169	810	0.37	1068	4404
M _o α = 0.9286	0.00035	3256	1042	0.32	1766	6003
M _o α = 0.9035	0.00033	3078	983	0.32	1671	5670
M _h α = 0.9286	0.00005	3256	1042	0.32	1766	6003
M _h α = 0.9035	0.00004	3078	983	0.32	1671	5669

Mad 2004-2006, Male-limited

Model	AICc	Delta AICc	AICc Weights	Model Likelihood	Num. Param.	Deviance
M_o α = 0.9035	-2249.333	0.0000	0.39132	1.0000	2	8.0460
M_o α = 0.9286	-2249.326	0.0067	0.39001	0.9966	2	8.0527
M _t α = 0.9286	-2245.450	3.8834	0.05614	0.1435	4	7.8997
M _t α = 0.9035	-2245.450	3.8835	0.05614	0.1435	4	7.8998
M _h α = 0.9035	-2245.304	4.0295	0.05218	0.1333	4	8.0460
M _h α = 0.9286	-2245.297	4.0362	0.05201	0.1329	4	8.0527
M _{th} α = 0.9286	-2237.578	11.7552	0.0011	0.0028	8	7.6609
M _{th} α = 0.9035	-2237.576	11.7572	0.0011	0.0028	8	7.6630

Model	Weight	N	SE	CV	LCL	UCL
M_o α = 0.9035	0.39132	4273	1565	0.37	2132	8564
M_o α = 0.9286	0.39001	4016	1469	0.37	2005	8043
M _t α = 0.9286	0.05614	4009	1466	0.37	2002	8029
M _t α = 0.9035	0.05614	4268	1563	0.37	2130	8554
M _h α = 0.9035	0.05218	4273	1565	0.37	2132	8565
M _h α = 0.9286	0.05201	4016	1469	0.37	2005	8043
M _{th} α = 0.9286	0.00110	4900	2732	0.56	1768	13583
M _{th} α = 0.9035	0.00110	4598	2415	0.53	1748	12097

APPENDIX III

Pradel Model using Photo-ID Data– Model outputs from Program MARK including AIC results and parameter estimates including, survival rate, Phi (ϕ), realized growth rate, Lambda (λ), capture probability (p) and the derived abundance (N) calculated by dividing capture probability into the sample size for each year (n_i/p_i). In each model p varies by sample occasion (t), and Phi and λ are either estimated as a constant (.) or fixed at values bracketing realistic expectations ($\phi=0.95, 0.98; \lambda=1.06, 1.10$).

Mad 2000-2006, excluding 2002						
Model	AICc	Delta AICc	AICc Weights	Model Likelihood	Num. Param.	Deviance
$\phi(.95)\lambda(1.10)p(t)$	3148.322	0.0000	0.23249	1.0000	6	35.9601
$\phi(.95)\lambda(1.06)p(t)$	3148.618	0.2967	0.20044	0.8621	6	36.2568
$\phi(.)\lambda(.)p(t)$	3149.070	0.7481	0.15994	0.6879	8	32.6346
$\phi(.98)\lambda(1.10)p(t)$	3149.304	0.9828	0.14223	0.6118	6	36.9429
$\phi(.98)\lambda(1.06)p(t)$	3149.655	1.3331	0.11938	0.5135	6	37.2932
$\phi(.95)\lambda(.)p(t)$	3150.241	1.9197	0.08903	0.3829	7	35.8454
$\phi(.98)\lambda(.)p(t)$	3151.151	2.8297	0.05649	0.2430	7	36.7554

$\phi(.95)\lambda(1.10)p(t)$										
Parameter	State	Estimate	SE	CV	LCL	UCL	n	N	LCL	UCL
ϕ	Fixed	0.95								
$p(2000)$		0.0173	0.00356	0.21	0.0115	0.0258	89	5155	3447	7732
$p(2001)$		0.0280	0.00543	0.19	0.0191	0.0409	159	5671	3888	8306
$p(2003)$		0.0184	0.00364	0.20	0.0124	0.0270	126	6861	4662	10127
$p(2004)$		0.0200	0.00389	0.19	0.0136	0.0293	151	7547	5162	11068
$p(2005)$		0.0173	0.00339	0.20	0.0118	0.0254	144	8302	5668	12193
$p(2006)$		0.0173	0.00336	0.19	0.0118	0.0253	158	9133	6253	13372
λ	Fixed	1.10								

$\phi(.95)\lambda(1.06)p(t)$										
Parameter	State	Estimate	SE	CV	LCL	UCL	n	N	LCL	UCL
ϕ	Fixed	0.95								
$p(2000)$		0.0146	0.00300	0.21	0.0097	0.0218	89	6109	4085	9159
$p(2001)$		0.0246	0.00476	0.19	0.0168	0.0358	159	6476	4440	9481
$p(2003)$		0.0173	0.00343	0.20	0.0117	0.0255	126	7276	4944	10736
$p(2004)$		0.0196	0.00381	0.19	0.0134	0.0286	151	7713	5276	11307
$p(2005)$		0.0176	0.00344	0.20	0.0120	0.0258	144	8176	5583	12004
$p(2006)$		0.0182	0.00353	0.19	0.0125	0.0266	158	8666	5936	12686
λ	Fixed	1.06								

$\phi(.)\lambda(.)p(t)$										
Parameter	State	Estimate	SE	CV	LCL	UCL	n	N	LCL	UCL
ϕ	Estimated	0.7464	0.10410		0.5004	0.8964				
$p(2000)$		0.0268	0.01552	0.58	0.0085	0.0812	89	3317	1096	10438
$p(2001)$		0.0449	0.02169	0.48	0.0171	0.1124	159	3544	1414	9289
$p(2003)$		0.0311	0.01126	0.36	0.0152	0.0626	126	4046	2012	8273
$p(2004)$		0.0349	0.01213	0.35	0.0176	0.0683	151	4323	2212	8596
$p(2005)$		0.0312	0.01171	0.38	0.0148	0.0644	144	4619	2238	9709
$p(2006)$		0.0320	0.01393	0.44	0.0135	0.0739	158	4936	2137	11692
λ	Estimated	1.0685	0.12866		0.8446	1.3518				

$\phi(.98)\lambda(1.10)p(t)$

Parameter	State	Estimate	SE	CV	LCL	UCL	<i>n</i>	<i>N</i>	LCL	UCL
ϕ	Fixed	0.98								
$p(2000)$		0.0159	0.00327	0.21	0.0106	0.0237	89	5602	3748	8397
$p(2001)$		0.0258	0.00499	0.19	0.0176	0.0376	159	6163	4226	9020
$p(2003)$		0.0169	0.00334	0.20	0.0115	0.0249	126	7457	5068	10999
$p(2004)$		0.0184	0.00358	0.19	0.0126	0.0269	151	8202	5612	12021
$p(2005)$		0.0160	0.00312	0.20	0.0109	0.0234	144	9023	6162	13243
$p(2006)$		0.0159	0.00308	0.19	0.0109	0.0232	158	9925	6799	14523
λ	Fixed	1.10								

 $\phi(.98)\lambda(1.06)p(t)$

Parameter	State	Estimate	SE	CV	LCL	UCL	<i>n</i>	<i>N</i>	LCL	UCL
ϕ	Fixed	0.98								
$p(2000)$		0.0134	0.00276	0.21	0.0089	0.0200	89	6646	4445	9957
$p(2001)$		0.0226	0.00437	0.19	0.0154	0.0329	159	7044	4831	10306
$p(2003)$		0.0159	0.00315	0.20	0.0108	0.0234	126	7915	5380	11671
$p(2004)$		0.0180	0.00350	0.19	0.0123	0.0263	151	8390	5742	12292
$p(2005)$		0.0162	0.00316	0.20	0.0110	0.0237	144	8893	6075	13050
$p(2006)$		0.0168	0.00324	0.19	0.0115	0.0245	158	9427	6460	13791
λ	Fixed	1.06								

 $\phi(.95)\lambda(.)p(t)$

Parameter	State	Estimate	SE	CV	LCL	UCL	<i>n</i>	<i>N</i>	LCL	UCL
ϕ	Fixed	0.95								
$p(2000)$		0.0207	0.01175	0.57	0.0068	0.0618	89	4294	1440	13175
$p(2001)$		0.0323	0.01464	0.45	0.0132	0.0772	159	4920	2061	12077
$p(2003)$		0.0195	0.00512	0.26	0.0116	0.0325	126	6457	3874	10819
$p(2004)$		0.0204	0.00412	0.20	0.0137	0.0303	151	7397	4990	11002
$p(2005)$		0.0170	0.00351	0.21	0.0113	0.0254	144	8474	5664	12716
$p(2006)$		0.0163	0.00436	0.27	0.0096	0.0274	158	9709	5758	16447
λ	Estimated	1.1456	0.13620		0.9082	1.4451				

 $\phi(.98)\lambda(.)p(t)$

Parameter	State	Estimate	SE	CV	LCL	UCL	<i>n</i>	<i>N</i>	LCL	UCL
ϕ	Fixed	0.98								
$p(2000)$		0.0201	0.01143	0.57	0.0065	0.0601	89	4426	1481	13609
$p(2001)$		0.0310	0.01407	0.45	0.0126	0.0742	159	5130	2144	12610
$p(2003)$		0.0183	0.00480	0.26	0.0109	0.0305	126	6891	4133	11548
$p(2004)$		0.0189	0.00381	0.20	0.0127	0.0280	151	7987	5389	11874
$p(2005)$		0.0156	0.00321	0.21	0.0104	0.0233	144	9258	6188	13886
$p(2006)$		0.0147	0.00395	0.27	0.0087	0.0248	158	10730	6359	18181
λ	Estimated	1.1590	0.13815		0.9183	1.4628				